Heavier Higgs particles: Indications from Minimal Supersymmetry

L. Maiani [a,*], A.D. Polosa [a], V. Riquer [b]

[a] *Dipartimento di Fisica, Sapienza Università di Roma, Piazzale A. Moro 5, Roma I-00185, Italy*
[b] *Fondazione TERA, Via G. Puccini 11, Novara I-28100, Italy*

A R T I C L E   I N F O

A B S T R A C T

We use the most recent data on the Higgs-like resonance h observed at 125 GeV to derive information about the mass of the heavier Higgs particles predicted by Minimal Supersymmetry. We treat as independent parameters the couplings of h to top quark, beauty and massive vector bosons and, in this three-dimensional space, we locate the point realizing the best fit to data and compare it to the position of the Standard Model point and to the region of coupling values accommodating heavier Higgs particles in Minimal Supersymmetry. We conclude that mass values $320 \lesssim M_H \lesssim 360$ GeV are compatible at 2σ with the best fit of couplings to present data, larger values being compatible at the 1σ level. Values of $1 \lesssim \tan\beta \lesssim 6$ are compatible with data.

In a recent paper [1], we confronted Minimal Supersymmetry for the Higgs sector with the particle discovered by ATLAS and CMS at 125 GeV. At that time, only the value of the mass was available, which, as noted also by other authors [2,3], is remarkably consistent with Minimal Supersymmetric Standard Model (MSSM), albeit with a value of the scalar top mass around 4 TeV. The presence of a tenuous bump at about 320 GeV in the CMS data for the ZZ channel could have been taken as a hint of the heavier, MSSM, 0^+ Higgs particle, H. With the higher statistics now available there is no trace left of such a structure.

In this Letter, we confront MSSM with the most recent data of the resonance $h(125)$ provided by ATLAS [4], CMS [5] and Tevatron [6]. Mass is given as

$$M_h = \begin{pmatrix} 126.0 \pm 0.4 \pm 0.4, & \text{ATLAS} \\ 125.3 \pm 0.4 \pm 0.5, & \text{CMS} \end{pmatrix} \quad (1)$$

For simplicity, we shall use in the computations of cross sections and decay rates the conventional value $M_h = 125$ GeV.

The experimental signals for decays are given by the ratios:

$$\mu_i = \frac{(\sigma_i \times \text{BR}_i)_{\text{expt}}}{(\sigma_i \times \text{BR}_i)_{\text{SM}}} \quad (2)$$

for the channels $i = WW, ZZ, b\bar{b}, \tau\bar{\tau}, \gamma\gamma$, for ATLAS [4] and CMS [5], and $i = b\bar{b}$ for Tevatron [6].

We aim to obtain limits on the mass of H and of its closeby partners A and $H^\pm$ and on the $\tan\beta$ parameter.

We find that, to one standard deviation, MSSM is consistent with present observation for $M_H \gtrsim 360$ GeV, and for $\tan\beta \gtrsim 1$.

We study the problem in the (c_t, c_b, c_W) space of couplings of the h resonance to the top and beauty quarks and to the vector bosons, c_i representing the ratios of the MSSM to the Standard Model (SM) couplings. We set $c_Z = c_W$ and use the same coupling c_t for all up fermions, *e.g.* charm, and c_b for all down fermions, *e.g.* τ.

Two different types of cross sections for the h production appear into the definition of μ_i given above, namely the gluon fusion cross section σ_{gf} and the vector boson fusion one, σ_{VBF}. These are parameterized according to

$$\sigma_{\text{gf}} = (\sigma_{\text{gf}})_{\text{SM}} c_t^2 \quad (3)$$

$$\sigma_{\text{VBF}} = (\sigma_{\text{VBF}})_{\text{SM}} c_W^2 \quad (4)$$

Cross section (3) is dominated by the top quark loop and it applies to the first four decay channels listed above. The cross section in (4) appears in the $\gamma\gamma$ channel due to the stringent cuts applied by ATLAS and CMS to the diphoton distribution so as to enhance the purity of the $\gamma\gamma$ signal. In this case we write

$$\bar{\sigma} = (\bar{\sigma}_{\text{gf}})_{\text{SM}} c_t^2 + (\bar{\sigma}_{\text{VBF}})_{\text{SM}} c_W^2 \quad (5)$$

where the bar represents the effect of the experimental cuts. The ratio $\bar{\sigma}/\bar{\sigma}_{\text{SM}}$ depends only on the ratio:

$$R = \frac{\bar{\sigma}_{\text{VBF}}}{\bar{\sigma}_{\text{gf}}} \quad (6)$$

In Ref. [1] one finds a detailed calculation of R at 7 TeV using ALPGEN [7] supplemented by the cuts specified by CMS in Ref. [8]. No difference using ATLAS cuts is found. We found $R = 2.97$ @ 7 TeV, whereas we find, with the same tools, $R = 3.1$ @ 8 TeV. Neglecting such a small deviation, we can use the cross sections computed

* Corresponding author.
E-mail address: luciano.maiani@cern.ch (L. Maiani).
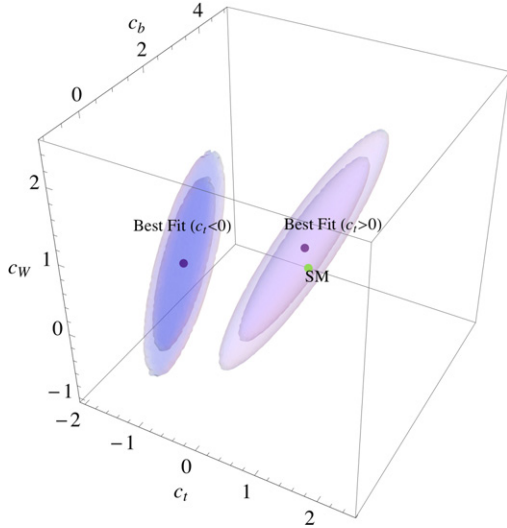
Fig. 1. 1σ (inner) and 2σ (outer) regions in the space (c_t, c_b, c_W) around the best fit points obtained by minimizing the χ^2 function. The fit includes ATLAS, CMS and Tevatron data, see text. Solutions are at $(\bar{c}_t, \bar{c}_b, \bar{c}_W)^+ = (0.886, 1.14, 1.19)$ and $(\bar{c}_t, \bar{c}_b, \bar{c}_W)^- = (-0.908, 0.642, 0.666)$. We also add a point for the Standard Model value (green point). (For interpretation of the references to color, the reader is referred to the web version of this Letter.)

in [1] to compare with the experimental values for μ_i, which are obtained by combining data at 7 and 8 TeV.

Widths in Vector–Vector and fermion antifermion decays of h are parameterized by rescaling the Standard Model values by the appropriate factors, c_W^2, etc. As for the $\gamma\gamma$ width, we write

$$\Gamma(\gamma\gamma) = \Gamma(\gamma\gamma)_{\text{SM}} \frac{|g_1 c_W + g_{1/2} c_t|^2}{|g_1 + g_{1/2}|^2} \tag{7}$$

where $g_{1,1/2}$ are the loop contributions of W and top [10], with

$$g_1 = 8.32, \qquad g_{1/2} = -1.84 \tag{8}$$

The total width is obtained from the sum of the individual widths, and branching ratios are obtained accordingly.

We discuss in the end the possible contribution of scalar top quarks in the gg and $\gamma\gamma$ loops. We anticipate however that the eventual effect of scalar top quarks in the loop simply amounts to a redefinition of c_t, leaving the structure of the above equations unchanged.[1]

To find the best fit values of the c's, we minimize the usual χ^2 function:

$$\chi^2 = \sum_a \frac{[\mu_a - G_a(c_t, c_b, c_W)]^2}{\sigma_a^2} \tag{9}$$

where μ_a runs over the values of μ, Eq. (2) given by ATLAS, CMS and Tevatron, σ_a the corresponding error and G_a the theoretical expressions introduced above in terms of the couplings. We have in all eleven experimental data and three parameters, namely eight degrees of freedom.

As a first step we identify the points in this space which minimize the χ^2 function. Setting conventionally $c_W \gtrsim 0$, we obtain the two solutions shown in Fig. 1, corresponding to $c_t < 0$ and $c_t > 0$. The two solutions have the same value of χ^2, with $\chi^2/\text{d.o.f.} = 0.6$.

---

[1] By using the same c_t in the $c\bar{c}$ width, we introduce a slight inaccuracy in the branching ratios via the total width, the charm cross section being a very minor component of it.

The relative sign of c_t and c_W is relevant to the $\gamma\gamma$ decay, see Eq. (7). It is no surprise that there is also a best fit solution with $c_t < 0$, particularly in a situation where the central $\gamma\gamma$ signal exceeds the SM value [4,5]. A similar situation was also found in recent two-parameter fits [9,11–13].

The inner and outer shells in Fig. 1 represent the 1σ and 2σ regions. In the same figure we place the Standard Model point $(1, 1, 1)$, which falls within 1σ from the best fit to data. We will focus on the positive solution.

Next we study the surface S: $(c_t(\tan\beta, m_H), c_b(\tan\beta, m_H), c_W(\tan\beta, m_H))$ predicted by Minimal Supersymmetry. Here we briefly recall its definition.

To start, let us recall that in the basis (H_d, H_u), the mass matrix of the CP-even Higgs fields is given by

$$\mathcal{M}_S^2 = M_Z^2 \begin{pmatrix} \cos^2\beta & -\cos\beta\sin\beta \\ -\cos\beta\sin\beta & \sin^2\beta \end{pmatrix}$$
$$+ M_A^2 \begin{pmatrix} \sin^2\beta & -\cos\beta\sin\beta \\ -\cos\beta\sin\beta & \cos^2\beta \end{pmatrix} + \begin{pmatrix} 0 & 0 \\ 0 & \delta \end{pmatrix} \tag{10}$$

with δ the radiative correction

$$\delta = \frac{3\sqrt{2}}{\pi^2 \sin^2\beta} G_F (M_t)^4 \log\left(\frac{\sqrt{M_{\tilde{t}_1} M_{\tilde{t}_2}}}{M_t}\right) \tag{11}$$

The first term in $\mathcal{M}_S^2$ arises from the so-called Fayet–Iliopoulos term determined by the gauge interaction. In the radiative corrections we have kept only the top-stop contribution. We determine the system of eigenvalues and eigenvectors of this matrix expressing M_A in terms of the CP-even Higgs boson mass, M_H, and the known values for M_Z and $M_h = 125$ GeV, according to

$$M_A^2 = M_H^2 + M_h^2 - M_Z^2 - \delta \tag{12}$$

The latter relation is obtained by equating the trace of $\mathcal{M}_S^2$ to $M_H^2 + M_h^2$ (the sum of eigenvalues).

In the calculation of eigenvalues and eigenvectors, we also express the quantity t, defined by

$$t = \log\left(\frac{\sqrt{M_{\tilde{t}_1} M_{\tilde{t}_2}}}{M_t}\right) \tag{13}$$

as a function of $\tan\beta$ and M_H, i.e. we find $t = F(\tan\beta, M_H)$. This can be obtained from the eigenvalue difference squared, $(M_H^2 - M_h^2)^2$. The function F arises as the solution of a second order equation. However, the other root is spurious, as it does not reproduce the degeneracy of the heavier Higgs boson masses as $M_H \to \infty$, see below, Eqs. (15). More on the function F can be found in [1].

In the literature, it is customary to use M_A as an independent parameter. Here, M_A is obtained from Eq. (12) and from the function $F(\tan\beta, M_H)$. In addition:
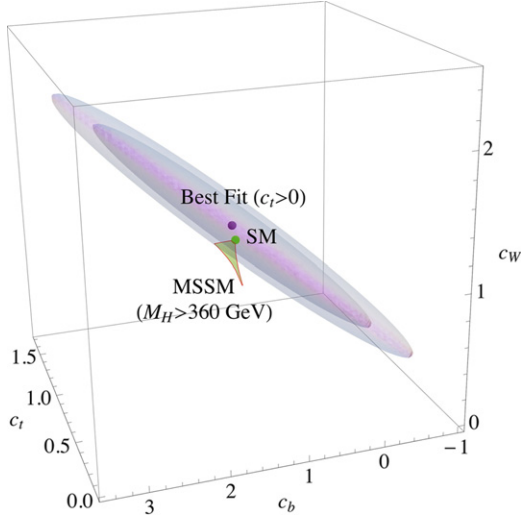
$$M_{H^\pm}^2 = M_A^2 + M_W^2 \tag{14}$$

For future reference, we record some values of M_A and $M_{H^\pm}$ (in GeV):

$$M_A = [315, 358]; \qquad M_{H^\pm} = [325, 367] \quad (M_H = 360)$$
$$M_A = [600, 619]; \qquad M_{H^\pm} = [604, 624] \quad (M_H = 620)$$
$$\tan\beta = [1, 6] \tag{15}$$

We next proceed to the computation of the normalized eigenvector corresponding to $h(125)$, namely:

$$\boldsymbol{S}_h(\tan\beta, M_H) = \begin{pmatrix} S_{hd}(\tan\beta, M_H) \\ S_{hu}(\tan\beta, M_H) \end{pmatrix} \tag{16}$$

Fig. 2. The intersection of the surface S in the (c_t, c_b, c_W) space, as predicted by MSSM, with the 1σ and 2σ regions around the best fit point to ATLAS and CMS data.

and define the surface S parameterized by $\tan\beta$ and M_H in the (c_t, c_b, c_W) space:

$$c_t(\tan\beta, M_H) = \frac{\sqrt{1 + \tan^2\beta}}{\tan\beta} S_{hu}(\tan\beta, M_H) \tag{17}$$

$$c_b(\tan\beta, M_H) = \sqrt{1 + \tan^2\beta}\, S_{hd}(\tan\beta, M_H) \tag{18}$$

$$c_W(\tan\beta, M_H) = \frac{1}{\sqrt{1 + \tan^2\beta}} S_{hd}(\tan\beta, M_H)$$
$$+ \frac{\tan\beta}{\sqrt{1 + \tan^2\beta}} S_{hu}(\tan\beta, M_H) \tag{19}$$

In Fig. 2 we show the 1σ and 2σ regions around the best fit solution with $c_t > 0$, intercepted by the surface S described above, in the parameter range:

$$320\,\text{GeV} < M_H < 620\,\text{GeV}; \quad 1 < \tan\beta < 6 \tag{20}$$

The so-called decoupling limit is manifested here in the fact that S heads straight into the Standard Model point as the mass M_H is increased. To be definite, we restrict to the mass range (20).

A better display of the situation is obtained by fixing $c_W = 1$ and considering the intersections of the 1σ, 2σ ellipsoids with that plane. This is illustrated in Fig. 3 where we also plot the surface S as embedded in the (c_t, c_b) space.

The (blue) points on the left side of S correspond to $M_H = 320$, 360 and 620 GeV, the intermediate value marking the border of the 1σ region. The (red) points crossing the surface from the left to the right are associated to different values of $\tan\beta$, from 1, at the lefthand side, to 6, at the righthand one. The best fit point projects inside the MSSM surface, but is above it ($\bar{c}_W = 1.19$) in the three-dimensional space.

The outcome of this analysis is that, even though we lost the footprints of a heavier Higgs at 320 GeV, the hypothesis that the second 0^+ particle predicted by Minimal Supersymmetry might just be lurking in the background is still viable.

To 1σ, the region $M_H \gtrsim 360$ GeV is all allowed, along with $1 < \tan\beta \lesssim 6$, consistently with the limits arising from the absence of Flavor Changing Neutral Current B_s decays. Data are compatible with a regime of incomplete decoupling, the 'intermediate-coupling regime' of Ref. [3]. However, MSSM could well be realized in the full decoupling mode. Consistency to 1σ with SM is also found in [14].
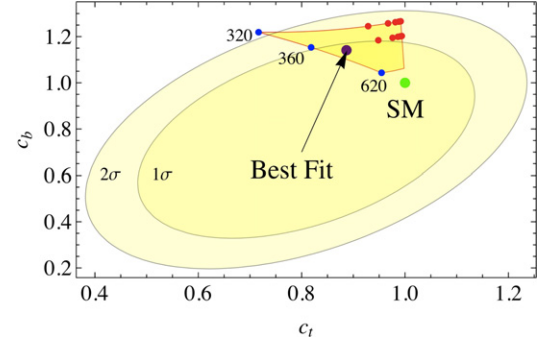
Fig. 3. The surface S as embedded in the (c_t, c_b) space at $c_W = 1$. The 1σ and 2σ regions are the intersections of the ellipsoids at $c_t > 0$, Figs. 1 and 2 with the plane $c_W = 1$. The outer side and the short inner side of S correspond to $M_H = 320$ and $M_H = 620$ GeV, respectively. The intersection with the 1σ border corresponds to $M_H = 360$ GeV. Red points mark values of $\tan\beta$ from 1 (lefthand side) to 6 (right-hand side). The best fit point projects inside the MSSM surface, but is above it ($\bar{c}_W = 1.19$) in the three-dimensional space. (For interpretation of the references to color, the reader is referred to the web version of this Letter.)
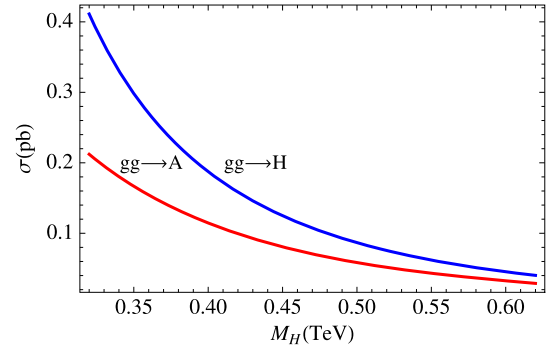
Fig. 4. Production of H and A at the LHC (total energy 8 TeV) from gluon fusion. Cross sections (pb) are given for $\tan\beta = 1.5$, as functions of M_H (TeV), in the 2σ allowed range.

In Ref. [1] we had reported the values of $\sigma \times$ BR for a hypothetical H at $M_H = 320$ and 500 GeV. We close here by giving the picture for M_H at 360 and 620 GeV and comment on production and decay of the corresponding pseudoscalar and charged Higgs particles, A and $H^\pm$.

Cross sections for H and A production by gluon fusion are shown in Fig. 4 in the full 2σ allowed mass range, $360 < M_H < 620$ GeV. Cross sections have been computed with ALPGEN [7], and corrected with the gluon K-factor taken from [15].
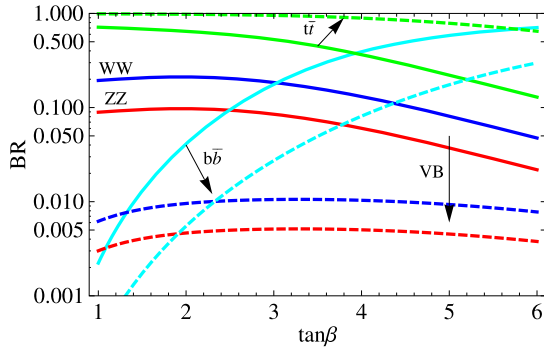
Branching ratios for the dominant decay channels of H are reported in Fig. 5, for $M_H = 360$ GeV, full lines, and $M_H = 620$ GeV, dashed lines, for $1 < \tan\beta < 6$. Decays are dominated by the $t\bar{t}$ channel, with vector boson and $b\bar{b}$ channels still visible in the lower part of the mass range.

A and $H^\pm$ decay branching ratios can be obtained with HDE-CAY [16]. In the 1σ allowed mass range, top quark channels, $t\bar{t}$ and $t\bar{b}$ respectively, are by far the dominant ones. Production at the LHC and decays of the $H^\pm$ have been extensively studied in Refs. [17]. The dominant mechanism, in the mass range considered here, is by b-gluon fusion:

$$b + g \rightarrow t + H^- \tag{21}$$

followed by $H^- \rightarrow \bar{t} + b$.

Finally, we comment on possible effects of scalar top quarks in the hgg and $h\gamma\gamma$ loops, in view of the large contribution of scalar tops to the Higgs mass correction, Eq. (11). Such effects have been considered in [18,19]. Unlike the mass correction, the $\gamma\gamma$ and gg loops are ultraviolet convergent, therefore heavy scalar particles

Fig. 5. Branching ratios for the dominant decay channels of H. Solid lines for $M_H = 360$ GeV, dashed ones for $M_H = 620$ GeV. Decays are dominated by the $t\bar{t}$ channel, whereas vector boson and $b\bar{b}$ channels are still visible in the lower part of the mass range.

decouple in the infinite mass limit. The only interesting case is the contribution of a light stop, the other one being correspondingly massive in order to satisfy Eq. (11). This case has been considered in [18] and leads, neglecting mixing among scalar quarks, to

$$\frac{A_{t+\tilde{t}}}{A_t} \approx 1 + \left(\frac{m_t}{M_{\tilde{t}_1}}\right)^2 \frac{A_0(\tau)}{A_{1/2}(\tau_t)}$$

$$\simeq 1 + 0.25 \left(\frac{m_t}{M_{\tilde{t}_1}}\right)^2 = f_t(M_{\tilde{t}_1}) \qquad (22)$$

where $\tau = 4M_{\tilde{t}_1}^2/m_h^2$ and $\tau_t = 4m_t^2/m_h^2$, and $A_{0,1/2}$ are defined in [18,19]. As noted before the additional contribution simply amounts to a redefinition of c_t and therefore does not affect the best fit procedure. In the no-mixing approximation, the $\tan\beta$ dependency of the top and scalar top loop amplitudes is the same so that the effect of scalar top simply leads to an effective loop t-quark coupling:

$$c_t^{\text{loop}}(\tan\beta, M_H) = f_t(M_{\tilde{t}_1})c_t(\tan\beta, M_H) \qquad (23)$$

This amounts to a 3% correction for $M_{\tilde{t}_1} = 500$ GeV.

In conclusion, present experimental information is consistent with the heavier scalar particles of MSSM to be in a relatively low energy region, between 320 and 620 GeV. A meaningful search can be done at the LHC, even at present luminosity. We underscore that higher Higgs particles still represent one of the most interesting test-tables of Minimal Supersymmetry.

References

[1] L. Maiani, A.D. Polosa, V. Riquer, New J. Phys. 14 (2012) 073029, arXiv: 1202.5998 [hep-ph].
[2] H. Baer, V. Barger, A. Mustafayev, Phys. Rev. D 85 (2012) 075010, arXiv: 1112.3017 [hep-ph].
[3] A. Arbey, M. Battaglia, A. Djouadi, F. Mahmoudi, arXiv:1207.1348 [hep-ph].
[4] G. Aad, et al., ATLAS Collaboration, Phys. Lett. B 716 (2012) 1, arXiv:1207.7214 [hep-ex], data used are the combined 7 and 8 TeV data reported in Fig. 10.
[5] S. Chatrchyan, et al., CMS Collaboration, Phys. Lett. B 716 (2012) 30, arXiv: 1207.7235 [hep-ex], data used are the combined 7 and 8 TeV data reported in Fig. 19.
[6] Tevatron New Physics Higgs Working Group and CDF and D0 Collaborations, arXiv:1207.0449 [hep-ex], data used are reported in Table VI, in correspondence to $m_h = 125$ GeV.
[7] M.L. Mangano, M. Moretti, F. Piccinini, R. Pittau, A.D. Polosa, JHEP 0307 (2003) 001, hep-ph/0206293.
[8] S. Chatrchyan, et al., CMS Collaboration, Phys. Rev. Lett. 108 (2012) 111804, arXiv:1202.1997 [hep-ex].
[9] A. Azatov, R. Contino, J. Galloway, arXiv:1206.3171 [hep-ph].
[10] W.J. Marciano, C. Zhang, S. Willenbrock, Phys. Rev. D 85 (2012) 013002, arXiv: 1109.5304 [hep-ph].
[11] J. Ellis, T. You, arXiv:1207.1693 [hep-ph].
[12] J.R. Espinosa, C. Grojean, M. Muhlleitner, M. Trott, arXiv:1207.1717 [hep-ph].
[13] M. Montull, F. Riva, arXiv:1207.1716 [hep-ph].
[14] J. Baglio, A. Djouadi, R.M. Godbole, Phys. Lett. B 716 (2012) 203, arXiv: 1207.1451 [hep-ph].
[15] http://www.pa.msu.edu/~huston/Kfactor/Kfactor.pdf.
[16] A. Djouadi, J. Kalinowski, M. Spira, Comput. Phys. Commun. 108 (1998) 56, hep-ph/9704448.
[17] T. Plehn, Phys. Rev. D 67 (2003) 014018, hep-ph/0206121;
S. Moretti, K. Odagiri, Phys. Rev. D 55 (1997) 5627, hep-ph/9611374;
V.D. Barger, R.J.N. Phillips, D.P. Roy, Phys. Lett. B 324 (1994) 236, hep-ph/9311372.
[18] A. Djouadi, Phys. Lett. B 435 (1998) 101, hep-ph/9806315.
[19] M. Carena, S. Gori, N.R. Shah, C.E.M. Wagner, JHEP 1203 (2012) 014, arXiv: 1112.3336 [hep-ph];
A more general analysis of the contribution of spin 0, 1/2, 1 particles in the loop is found in: M. Carena, I. Low, C.E.M. Wagner, JHEP 1208 (2012) 060, arXiv:1206.1082 [hep-ph].